Extended data file:

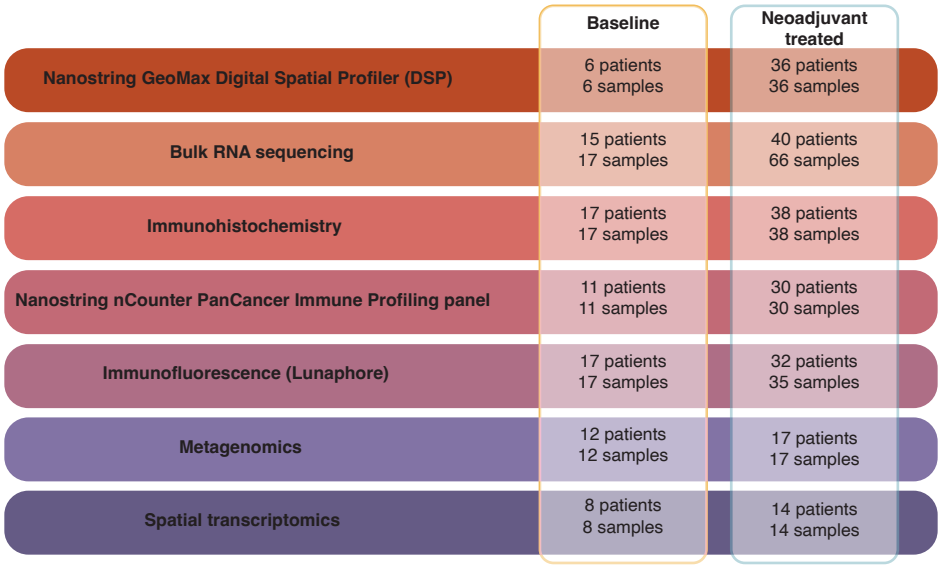
Baseline
Neoadjuvant treated
Nanostring GeoMax Digital Spatial Profiler (DSP)
6 patients
6 samples
36 patients
36 samples
Bulk RNA sequencing
15 patients
17 samples
40 patients
66 samples
Immunohistochemistry
17 patients
17 samples
38 patients
38 samples
Nanostring nCounter PanCancer Immune Profiling panel
11 patients
11 samples
30 patients
30 samples
Immunofluorescence (Lunaphore)
17 patients
17 samples
32 patients
35 samples
Metagenomics
12 patients
12 samples
17 patients
17 samples
Spatial transcriptomics
8 patients
8 samples
14 patients
14 samples

Supplementary Figure 1. Allocation of clinical trial samples. These samples were collected as part of two clinical trials of neo-adjuvant immunotherapy in cutaneous squamous cell carcinoma patients - NCT03565783 and NCT04154943. Figures represent number of patients with available specimen and the total number of specimens sent for analysis. Please note that for some assays more than one sample per patient were processed.

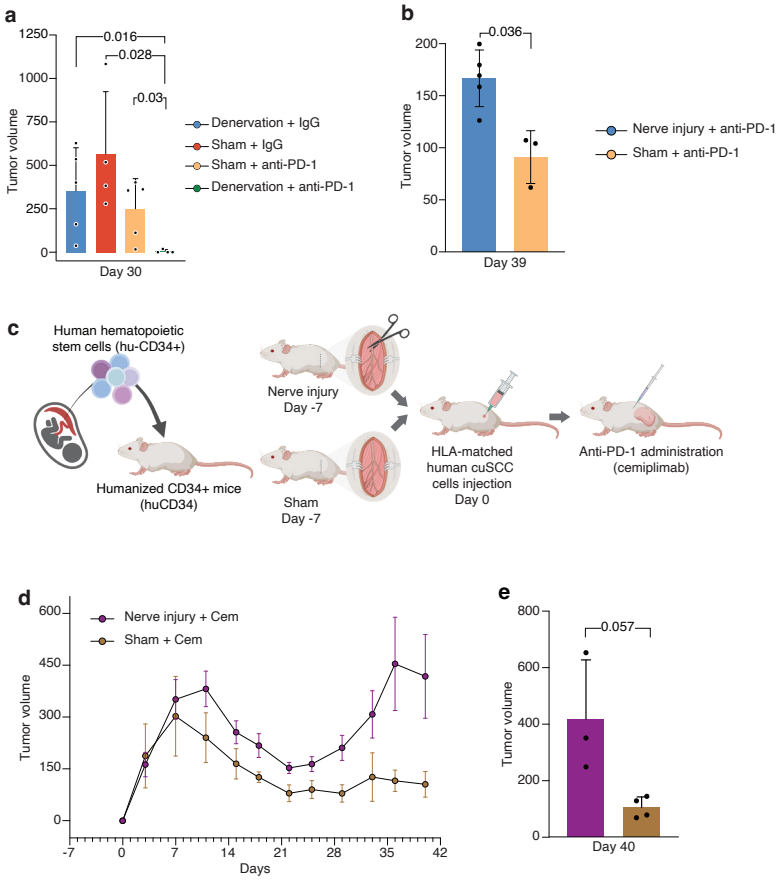
a
1250
1000
750
500
250
0
Tumor volume
0.016
0.028
0.03
Day 30
Denervation + IgG
Sham + IgG
Sham + anti-PD-1
Denervation + anti-PD-1
b
200
150
100
50
0
Tumor volume
0.036
Day 39
Nerve injury + anti-PD-1
Sham + anti-PD-1
c
Human hematopoietic
stem cells (hu-CD34+)
Humanized CD34+ mice
(huCD34)
Nerve injury
Day -7
Sham
Day -7
HLA-matched
human cuSCC
cells injection
Day 0
Anti-PD-1 administration
(cemiplimab)
d
600
450
300
150
0
Tumor volume
Nerve injury + Cem
Sham + Cem
-7
0
7
14
21
28
35
42
Days
e
800
600
400
200
0
Tumor volume
0.057
Day 40

Supplementary Figure 2. Neuromodulated humanized mouse experiments with the trial drug (cemiplimab). (a) Tumor volume bar plot of the denervation mouse model at day 30 (Kruskal-Wallis test). All animals in the denervation + Anti-PD-1 (cemiplimab) group, had either complete or major tumor resolution at day 30. **(b)** Tumor volume bar plot of the nerve injury experiment at day 39 **(c)** experiment design description of the nerve injury experiment in HLA matched humanized huCD34+ NSG mice. underwent axotomy to induce nerve injury or sham surgery. 7 days following surgical axonotomy (inducing nerve damage), the mice were injected orthotopically with HLA-matched human cuSCC cells. Anti-PD-1 treatment (Cemiplimab, same medication that was used in the clinical trial) was administered biweekly, starting 7 days after tumor implantation. **(d)** Tumor growth plot for the experiment described in (c). **(e)** Tumor volume bar plot of the same experiment, at day 40.

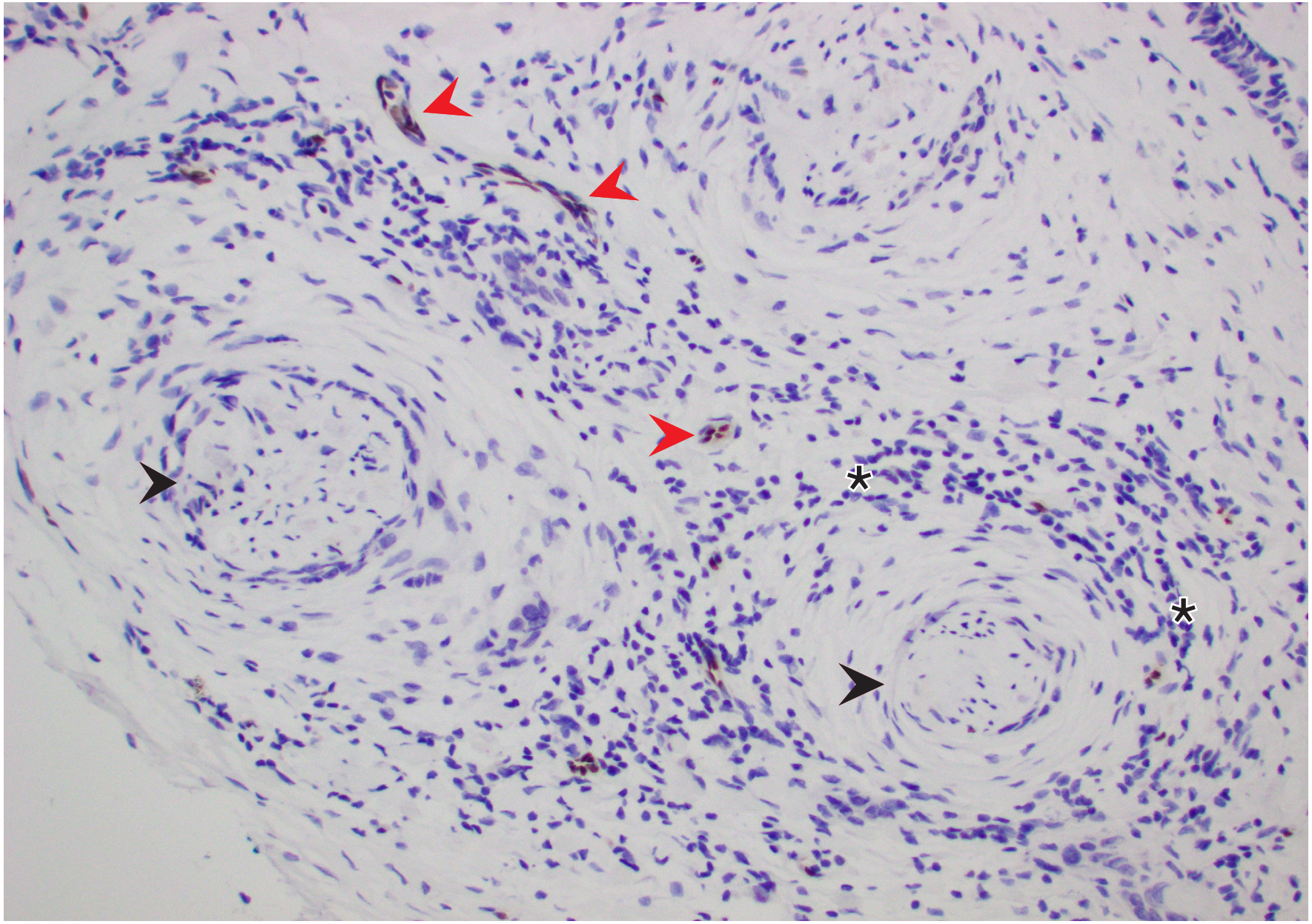

Supplementary Figure 3. Assessment on vascular integrity in the setting of nerve damage. Immunohistochemistry stain against ERG, marker for endothelial cells, conduct on tumor samples of an independent cutaneous squamous cell carcinoma (cSCC) patients with evidence of nerve damage and de-myelination (n = 86; see main text Figure 2). This representative stain against ERG showed intact intratumoral vasculature (red arrowheads, see vascular lumen integrity), and perineuroal inflammation (asterisks) suggesting that the tumor-associated nerve damage (nerve marked with black arrowheads) and perineural inflammation was not accompanied by vascular damage.

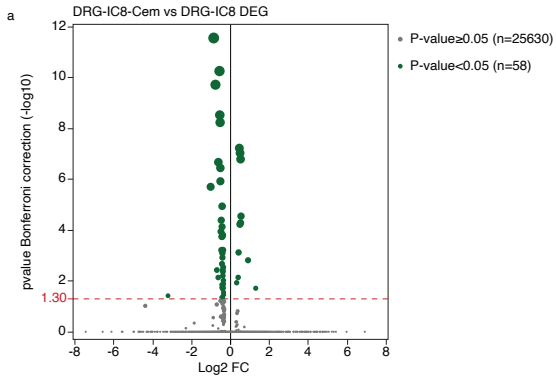
a
DRG-IC8-Cem vs DRG-IC8 DEG
P-value≥0.05 (n=25630)
P-value<0.05 (n=58)
pvalue Bonferroni correction (-log10)
1.30
Log2 FC

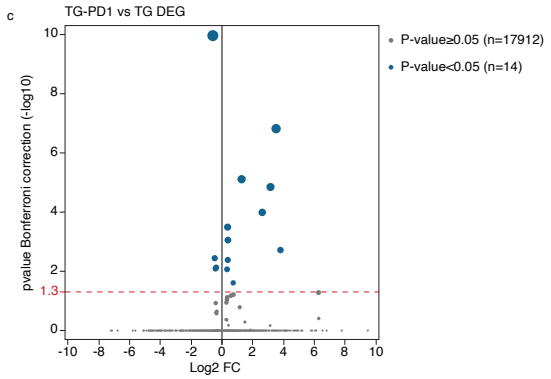
c
TG-PD1 vs TG DEG
P-value≥0.05 (n=17912)
P-value<0.05 (n=14)
pvalue Bonferroni correction (-log10)
1.3
Log2 FC

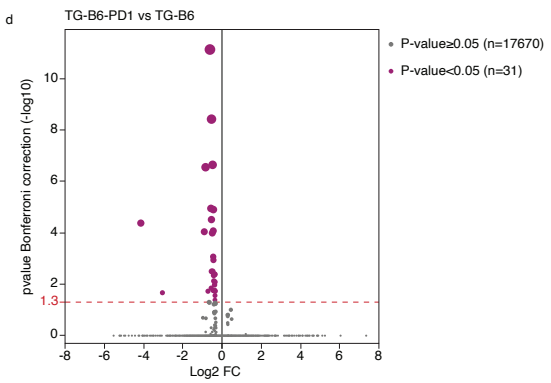
d
TG-B6-PD1 vs TG-B6
P-value≥0.05 (n=17670)
P-value<0.05 (n=31)
pvalue Bonferroni correction (-log10)
1.3
Log2 FC

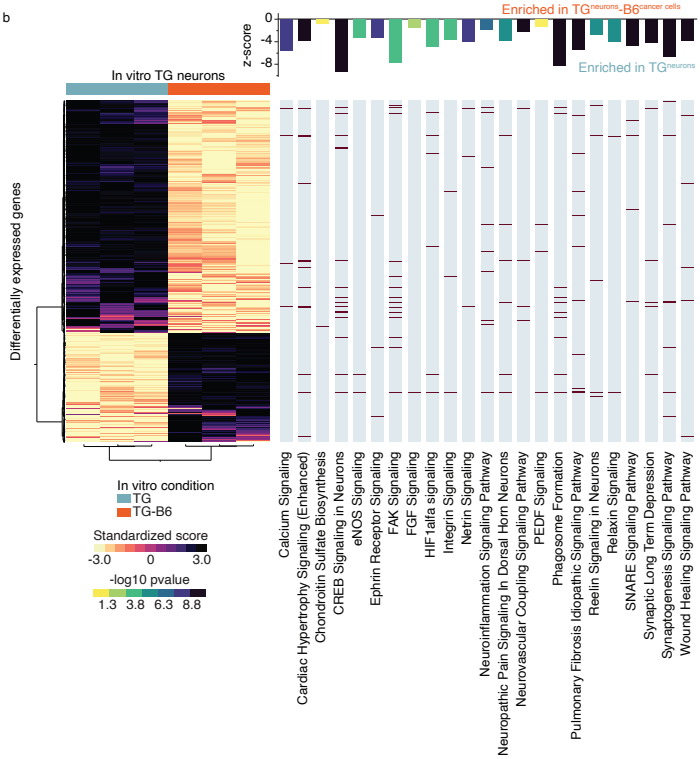
b
Enriched in TGneurons-B6cancer cells
z-score
Enriched in TGneurons
In vitro TG neurons
Differentially expressed genes
In vitro condition
TG
TG-B6
Standardized score
-3.0
0
3.0
-log10 pvalue
1.3 3.8 6.3 8.8
Calcium Signaling
Cardiac Hypertrophy Signaling (Enhanced)
Chondroitin Sulfate Biosynthesis
CREB Signaling in Neurons
eNOS Signaling
Ephrin Receptor Signaling
FAK Signaling
FGF Signaling
HIF1alfa signaling
Integrin Signaling
Netrin Signaling
Neuroinflammation Signaling Pathway
Neuropathic Pain Signaling In Dorsal Horn Neurons
Neurovascular Coupling Signaling Pathway
PEDF Signaling
Phagosome Formation
Pulmonary Fibrosis Idiopathic Signaling Pathway
Reelin Signaling in Neurons
Relaxin Signaling
SNARE Signaling Pathway
Synaptic Long Term Depression
Synaptogenesis Signaling Pathway
Wound Healing Signaling Pathway

Supplementary Figure 4. Murine trigeminal ganglia (TG) and human dorsal root ganglia (DRG) neurons share similar cancer-driven neural damage transcriptomics alteration. (a) Volcano plot showing the differential gene expression in DRG neurons co-cultured for 5 days with human IC8 cutaneous squamous cell carcinoma (sSCC) cells versus DRG neurons co-cultured IC8 SCC cells and anti-PD-1 (Cemiplimab, Cem). Only 58 genes out of 25,688 overall identified genes were differentially expressed in the presence of anti-PD-1; *P* values determined by two-sided Kruskal-Wallis rank-sum test and *q* value calculated by FDR. Please see Main Text Figure 2 and Supplementary Table 2 for additional details. **(b)** Heat map of differentially expressed genes between murine SKH primary TG neurons alone and TG neurons co-cultured with murine B6 cSCC. Enriched pathways (Ingenuity Pathway Analysis software – IPA) and their respective z-scores, p-values, and genes are shown on the left. **(c-d)** Volcano plot showing the differential gene expression in murine TG neurons versus TG neurons treated with anti-PD-1 (c) and TG neurons co-culture with B6 cSCC cells with versus without anti-PD-1 (d). All experiments were done in triplicates.

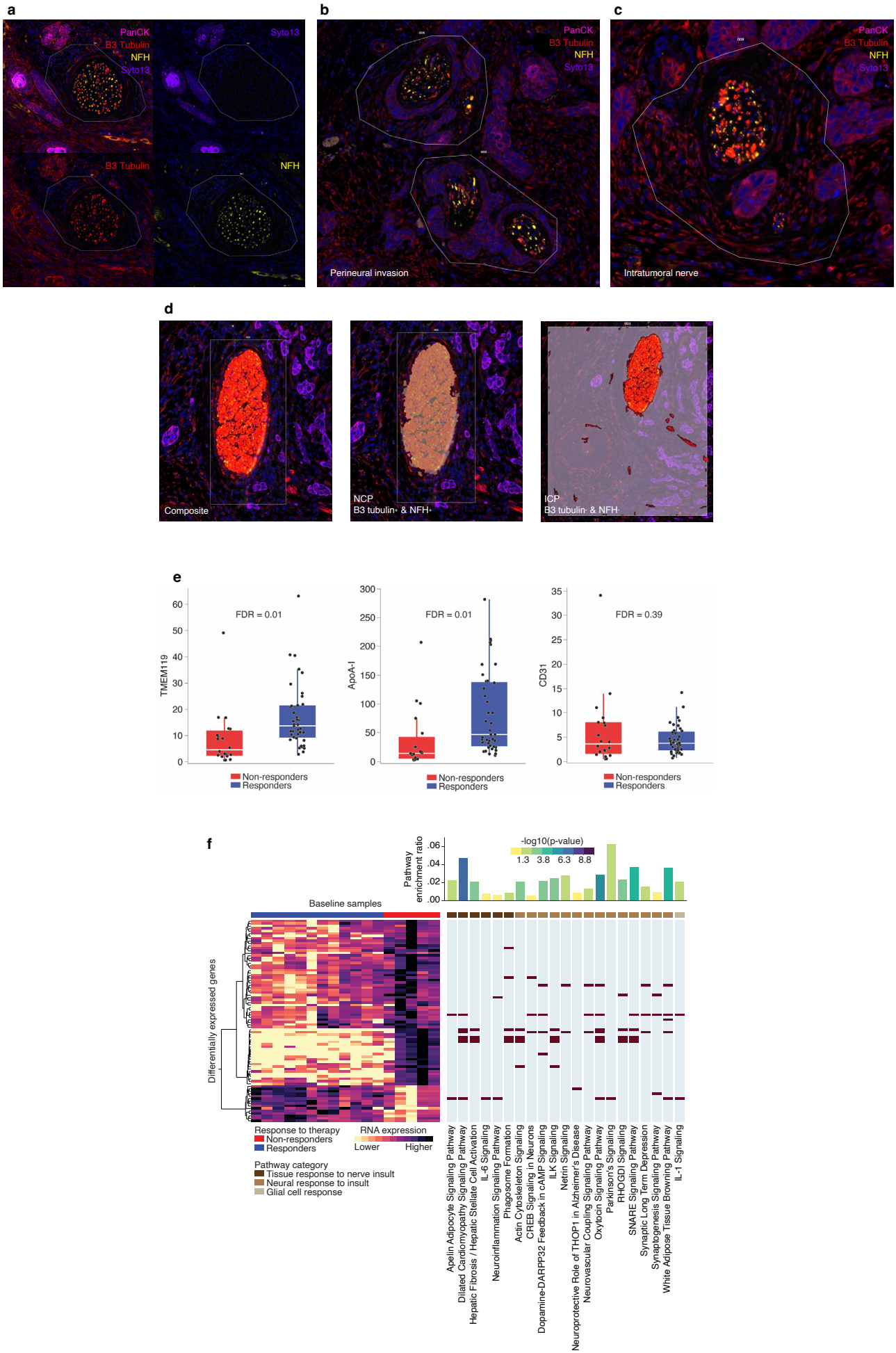
a
PanCK
B3 Tubulin
NFH
Syto13
B3 Tubulin
Syto13
NFH
b
PanCK
B3 Tubulin
NFH
Syto13
Perineural invasion
c
PanCK
B3 Tubulin
NFH
Syto13
Intratumoral nerve
d
Composite
NCP
B3 tubulin+ & NFH+
ICP
B3 tubulin- & NFH-
e
TMEM119
FDR = 0.01
ApoA-I
FDR = 0.01
CD31
FDR = 0.39
Non-responders
Responders
f
Pathway enrichment ratio
-log10(p-value)
1.3 3.8 6.3 8.8
Baseline samples
Differentially expressed genes
Response to therapy
Non-responders
Responders
RNA expression
Lower
Higher
Pathway category
Tissue response to nerve insult
Neural response to insult
Glial cell response
Apelin Adipocyte Signaling Pathway
Dilated Cardiomyopathy Signaling Pathway
Hepatic Fibrosis / Hepatic Stellate Cell Activation
IL-6 Signaling
Neuroinflammation Signaling Pathway
Phagosome Formation
Actin Cytoskeleton Signaling
CREB Signaling in Neurons
Dopamine-DARPP32 Feedback in cAMP Signaling
ILK Signaling
Netrin Signaling
Neuroprotective Role of THOP1 in Alzheimer's Disease
Neurovascular Coupling Signaling Pathway
Oxytocin Signaling Pathway
Parkinson's Signaling
RHOGDI Signaling
SNARE Signaling Pathway
Synaptic Long Term Depression
Synaptogenesis Signaling Pathway
White Adipose Tissue Browning Pathway
IL-1 Signaling

Supplementary Figure 5. Spatial protein analysis of peri-neural niches in tumor samples from our clinical trials cohort and transcriptomic validation of neurodegenerative signatures. (a-c) Representative images of nerve identification process for digital spatial profiling (DSP) analysis. Nerves were identified using neurofilament heavy chain (NFH, yellow) and B3-tubulin (red) staining neoadjuvant-treated tumor samples of a responder **(a)** and non-responder (**b-c**); note the pan-cytokeratin (PanCK)-positive cancer cells (in pink) encircling the nerve. The white line outlines the geometric region of interest that was analyzed for protein expression using DSP. Original magnification, ×40. **(d)** Geometric region of interest (ROI, white rectangle) showing a representative digital capture of the nerve (middle, shadowed, nerve capture panel, NCP) and the surrounding peri-neural niche which was assessed for immune markers (left, shadowed, immune capture panel, ICP). The former was analyzed for neural phenotypic markers and the latter for immune markers. **(e)** Box plots showing expression levels of neuro-protective markers (TMEM119 and ApoA-1) and marker of blood-nerve barrier reactivity and angiogenesis (CD31, representing disrupted blood-nerve barrier following nerve damage) in tumor-associated nerves (TANs) among baseline tumor samples according to clinical response status. White lines represent median values, and error bars represent interquartile ranges; black dots represent individual samples. N = 118 niches; FDR, false discovery rate. **(f)** Transcriptional differences between responders and non-responders to anti-PD-1 therapy in baseline tumor samples (bulk RNA sequencing). The heatmap shows genes involved in mechanisms of degeneration and survival of neurons. Unsupervised hierarchical clustering analysis (HCA) shows the differentially expressed genes (DEG) between responders and non-responders. The pathway analysis results (Ingenuity Pathway Analysis, QIAGEN) are shown according to their z-scores and p-values (Fisher's Exact test). DEG belonging to the depicted enriched pathways are highlighted (brown) in the adjacent chart.

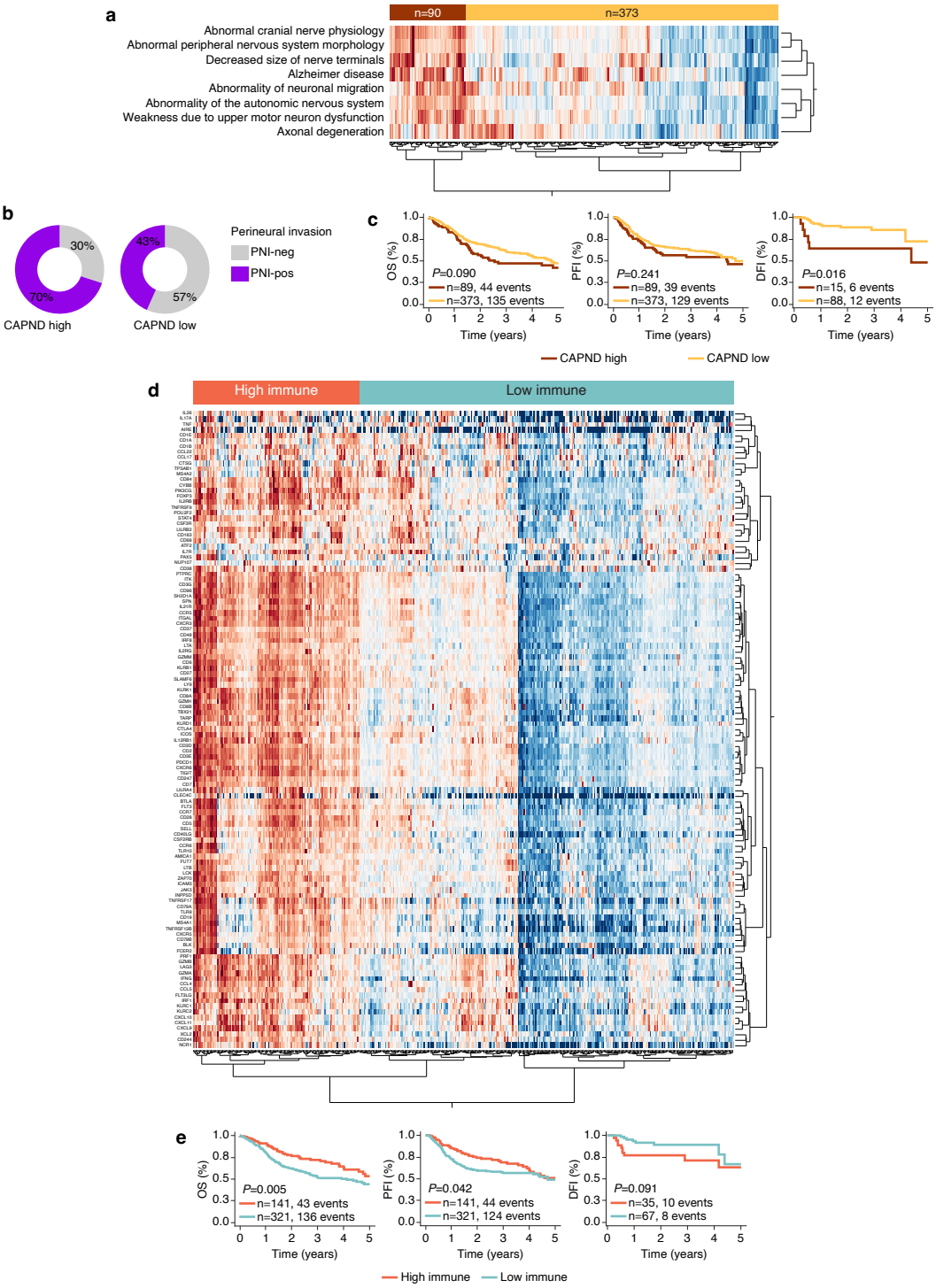
a
n=90
n=373
Abnormal cranial nerve physiology
Abnormal peripheral nervous system morphology
Decreased size of nerve terminals
Alzheimer disease
Abnormality of neuronal migration
Abnormality of the autonomic nervous system
Weakness due to upper motor neuron dysfunction
Axonal degeneration
b
30%
70%
CAPND high
43%
57%
CAPND low
Perineural invasion
PNI-neg
PNI-pos
c
OS (%)
P=0.090
n=89, 44 events
n=373, 135 events
PFI (%)
P=0.241
n=89, 39 events
n=373, 129 events
DFI (%)
P=0.016
n=15, 6 events
n=88, 12 events
Time (years)
CAPND high
CAPND low
d
High immune
Low immune
e
OS (%)
P=0.005
n=141, 43 events
n=321, 136 events
PFI (%)
P=0.042
n=141, 44 events
n=321, 124 events
DFI (%)
P=0.091
n=35, 10 events
n=67, 8 events
Time (years)
High immune
Low immune

Supplementary Figure 6. Cancer associated peripheral nerve degeneration (CAPND) is associated with worse survival in an external TCGA cohort of mucosal head and neck squamous cell carcinoma patients (HNSCC). (a) Unsupervised hierarchical clustering analysis (HCA) using single sample enrichment scores for CAPND related gene sets among TCGA HNSCC patients. The gene sets presented were enriched among non-responding tumor samples from our clinical trial cohort (see Main Figure Text 2). The enrichment scores were determined by single sample Gene Set Enrichment Analyses (ssGSEA) considering selected gene sets from the Human Phenotype Ontology (HPO) database. The HCA identified two groups characterized by distinct expression of CAPND related genes – high (CAPND - enriched) and low expression (CAPND non-enriched). **(b)** The perineural invasion (PNI) status among tumors TCGA HNSCC patients based on their CAPND scores. PNI was detected in 70% (n=49, out of 70) of the tumors in the CAPND-high group, and only in 43.4% (n=111, out of 256) of the CAPND-low group (Fisher's exact test p-value<0.0001), demonstrating as association between functional evidence of nerve damage (CAPND score) and morphological one (PNI). **(c)** Kaplan-Meier analysis of overall survival (OS), progression-free interval (PFI), and disease-free interval (DFI) by CAPND scores group (red – high score, yellow – low score). **(d)** HCA of TCGA HNSCC RNA-seq data using a curated list of genes associated with immune activity[1] in head and neck cancer, identified two groups with distinct immune activity – high (red) versus low (teal). **(e)** Kaplan-Meier estimates of overall survival (OS), progression-free interval (PFI), and disease-free interval (DFI) of the TCGA HNSCC patients stratified by the immune signature groups. All p values for survival rate differences were calculated using Log-rank analysis.

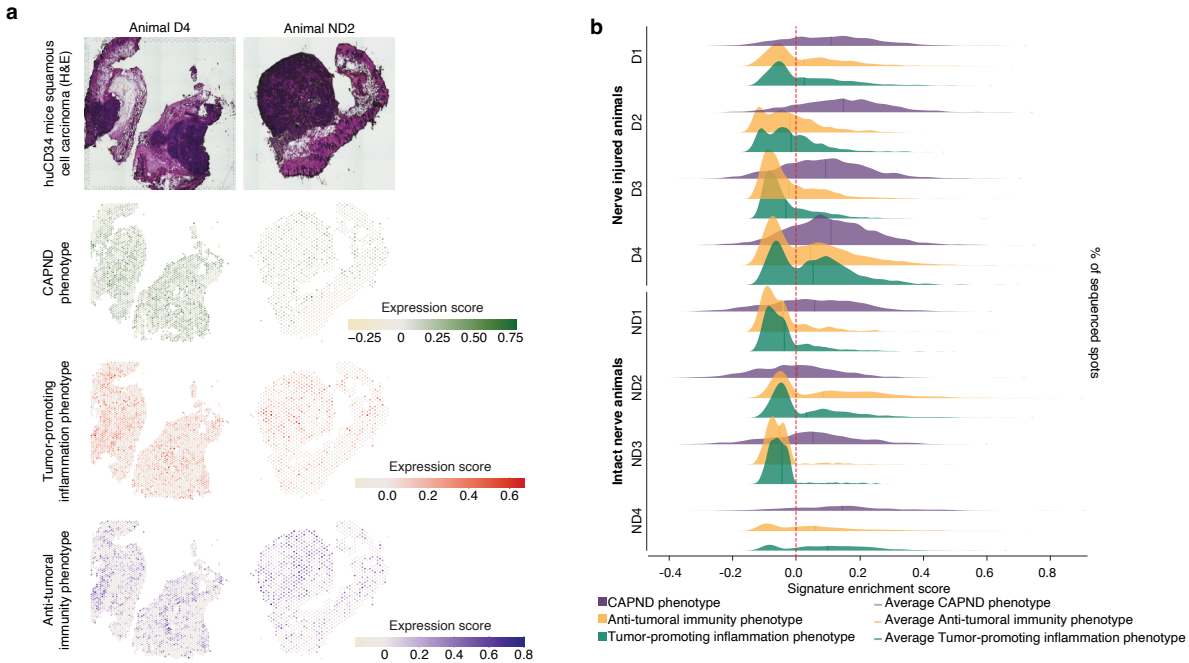
a
Animal D4
Animal ND2
huCD34 mice squamous cell carcinoma (H&E)
CAPND phenotype
Expression score
−0.25 0 0.25 0.50 0.75
Tumor-promoting inflammation phenotype
Expression score
0.0 0.2 0.4 0.6
Anti-tumoral immunity phenotype
Expression score
0 0.2 0.4 0.6 0.8
b
Nerve injured animals
D1
D2
D3
D4
Intact nerve animals
ND1
ND2
ND3
ND4
% of sequenced spots
-0.4 -0.2 0.0 0.2 0.4 0.6 0.8
Signature enrichment score
CAPND phenotype
Anti-tumoral immunity phenotype
Tumor-promoting inflammation phenotype
Average CAPND phenotype
Average Anti-tumoral immunity phenotype
Average Tumor-promoting inflammation phenotype

Supplementary Figure 7. Spatial transcriptomics data from humanized mice nerve injury experiment. (a) Eight tumor samples from huCD34^{+} NSG mice with (n=4) and without (n=4) nerve injury were used for spatial transcriptomic analysis evaluating human and murine genes. This analysis assessed the co-localization of three phenotypes: Cancer associated peripheral nerve degeneration (CAPND), tumor-promoting inflammation, and anti-tumoral immunity. Phenotypes were established based on human genes (see Main Text Figure 3). Representative images and their respective sequenced spots are shown for tumors samples from a nerve-injured mice (D4) and a control mice (ND2). **(b)** The ridgeplot shows the frequency distribution of sequenced tissue spots (y-axis) at a given enrichment score (x-axis, right to the red line) for each sample and each phenotype signature. Nerve injured animals (D1-4) show concomitant increase of CAPND (purple, >0 values) and tumor-promoting inflammation (green) phenotypes compared to animals without nerve injury (ND1-4). Note that while all tumors has nerve injury to some extent, the injured ones (top four) has significantly higher CAPND enrichment.

Extended figure 9

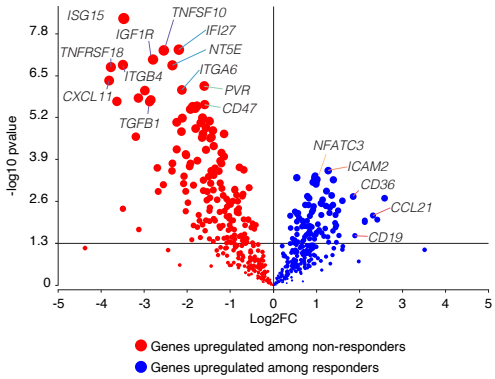

Supplementary Figure 8. Assessment of intra-tumoral immune infiltration via Nanostring. Nanostring nCounter PanCancer analysis was performed on neoadjuvant-treated tumor samples of our clinical trial patients. The volcano plot demonstrates differentially expressed genes among responders (blue, n = 33) and non-responders (red, n =7). A similar analysis was not done for baseline samples due to a small samples size (baseline non-responder n=1). Please see Main Text Figure 4 for additional Nanostring analyses.

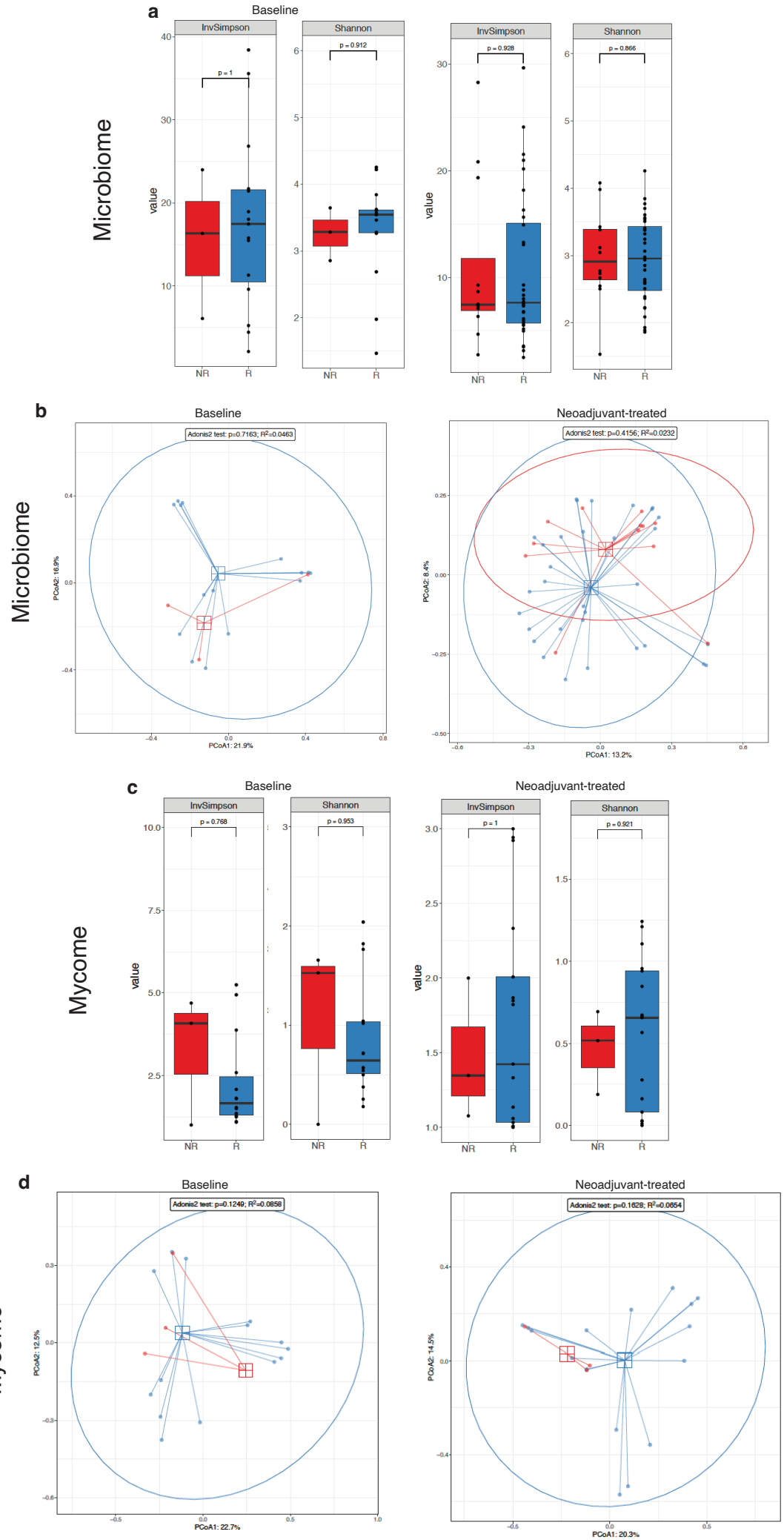
a
Baseline
Microbiome
InvSimpson
Shannon
p = 1
p = 0.912
p = 0.928
p = 0.866
value
NR
R
b
Baseline
Neoadjuvant-treated
Microbiome
Adonis2 test: p=0.7163; R²=0.0463
Adonis2 test: p=0.4156; R²=0.0232
PCoA1: 21.9%
PCoA2: 16.9%
PCoA1: 13.2%
PCoA2: 8.4%
c
Baseline
Neoadjuvant-treated
Mycome
InvSimpson
Shannon
p = 0.768
p = 0.953
p = 1
p = 0.921
value
NR
R
d
Baseline
Neoadjuvant-treated
Mycome
Adonis2 test: p=0.1249; R²=0.0858
Adonis2 test: p=0.1628; R²=0.0654
PCoA1: 22.7%
PCoA2: 12.5%
PCoA1: 20.3%
PCoA2: 14.5%

Supplementary Figure 9. Assessment of intra-tumoral micro-organisms and their potential association to response to anti-PD-1 therapy. (a) Alpha diversity analysis of intra-tumoral microbiome showing lack of significant difference between responders (R, blue) versus non-responders (NR, red) based on two different tests (Shannon and Inversed Simpson). **(b)** Beta diversity analysis using Bray distance test showing lack of differences in the composition of intra-tumoral microbiome communities between R and NR. **(c)** Alpha diversity analysis of intra-tumoral mycome (fungi) showing lack of significant difference between R and NR. **(d)** Beta diversity analysis using Bray distance test showing lack of differences in the composition of intra-tumoral mycome (fungi) communities between R and NR. Of note, the microbiome analysis was limited due to small sample size, especially among baseline tumor sample (n=3), and low reads. To avoid further data loss, the data did not undergo rarefaction before proceeding to the alpha and beta analysis.

References:

1 Prat, A. *et al.* Immune-Related Gene Expression Profiling After PD-1 Blockade in Non-Small Cell Lung Carcinoma, Head and Neck Squamous Cell Carcinoma, and Melanoma. *Cancer Res* **77**, 3540-3550, doi:10.1158/0008-5472.Can-16-3556 (2017).